Polypyrrole Asymmetric Bilayer Artificial Muscle: Driven Reactions, Cooperative Actuation, and Osmotic Effects

*Masaki Fuchiwaki, Jose G. Martinez, and Toribio F. Otero**

The coulo-dynamic (angle/consumed charge) characterization of an asymmetric polypyrrole (PPy) bending bilayer (PPy_1/PPy_2) muscle is performed in aqueous solutions by cyclic voltammetry with parallel video recording of a reversible angular displacement of 200°. The characterization of each of the two PPy_1/tape, PPy_2/tape muscles, describing 30° and 50° per voltammetric cycle, corroborates the driven muscle reactions and ionic exchanges. The asymmetric bilayer efficiency, as described degrees per reaction unit, is seven and four times that of the PPy/tape muscles. A cooperative electro-chemo-mechanical actuation of each of the individual layers occurs in the asymmetric bilayer. Each of the three muscles is a Faradaic polymeric motor: described angles are linear functions of the consumed charge with small hysteresis loops. Each loop is related to dynamic water osmotic balance following the reaction driven film swelling or its fast electro-osmotic expulsion around the reduction induced conformational closing and film compaction.

1. Introduction

Scientists, engineers, and tool/robot designers are developing a great activity trying to produce zoomorphic and anthropomorphic robots using soft and wet motors working in a similar way as natural muscles do. Inorganic, organic, polymeric, and carbon-based structures (carbon nanotubes, graphenes) respond to electric fields or to electrical charges with volume variations (electromechanical or electro-chemo-mechanical actuators, respectively). Electromechanical actuators require several volts (kV cm^{-1}) for actuation.[1,2] Electro-chemo-mechanical artificial muscles are polymeric motors driven by reversible electrochemical reactions (Faradaic motors) generating reversible volume variations required to lodge/expel balancing counterions and water.[3,4] A few mV of positive or negative potential increments reverse both, actuation movement and driving reaction.

Dr. M. Fuchiwaki
Department of Mechanical Information Science and Technology
Kyushu Institute of Technology
680–4, Kawazu, Iizuka (Fukuoka) 820–8502, Japan
J. G. Martinez, Prof. T. F. Otero
Center for Electrochemistry and Intelligent Materials
Universidad Politécnica de Cartagena
Aulario II, C/ Carlos III, s/n
Cartagena 30203, Spain
E-mail: toribio.fotero@upct.es

DOI: 10.1002/adfm.201404061

Artificial muscles from conducting polymers (CPs) are full reliable Faradaic motors: the rate of the movement is under linear control of the flowing current (charge per unit of time, or number of exchanged ions per unit of time) and the described angle is under linear control of the consumed charge.[5,6] They are full reproducible: whatever the dimensions or the CP content the same charge per unit of CP weight produces in the same electrolyte a constant displacement.[5–7] When its Faradaic (chemical) nature is ignored, very complex mathematical, physical or thermodynamic models are being developed in order to try to describe both, movement rate and movement position.[8–26] In addition the driving reaction senses (simultaneously to de actuation) any mechanical, thermal, or chemical change on the working conditions. Those dual sensing-motors open a new and unexplored world of artificial proprioceptive devices,[27–33] products, and robots.

Bending bilayers (CP/tape,[34,35] CP/metal,[36–38] CP/plastic,[39] interpenetrated polymer networks[40,41] are one of the most efficient structures transducing reaction driven small volume variations in the CP film to large (> ±30°) bending movements and macroscopic mechanical energy. The second layer (tape, metal, plastic) is required to translate the volume variation induced in the CP film by its reaction into mechanical stress gradient across the bilayer, origin of the macroscopic bending movement. Thus, the second layer is a passive layer that must be bended and trailed consuming energy during actuation.

Some asymmetric bilayers constituted by two different conducting polymers, CP_1/CP_2 (the two layer muscles are reactive) have been described in the literature.[42–50] Here we will look for cooperative and synergic electro-chemo-mechanical effects constructing and checking an asymmetric bilayer by selecting two asymmetric CP films: one of the films must allow to those families of CPs that swell during oxidation by entrance of anions and the second films must allow to those families of CPs that shrink during oxidation by expulsion of cations.[3,4,51] A PPy-ClO_4 film (PPy electrogenerated in presence of a ClO_4^- salt) is the expected anion exchange layer during oxidation/reduction[52,53] and a PPy-DBS (PPy electrogenerated in presence of a dodecyl benzyl sulphonate salt) is the expected cation exchange layer during oxidation/reduction.[52,54] The subsequent coulo-dynamic (angle vs consumed charge, α/Q) characterization of the PPy-ClO_4/PPy-DBS asymmetric bilayer muscle submitted to a

voltammetric control and the parallel coulo-dynamic characterization of each of the PPy-ClO_4/tape and PPy-DBS/tape bilayer muscles in NaBr aqueous solutions will corroborate the reaction driven ionic exchange (actuation) in each of the PPy layer and the quantification of the expected cooperative actuation.

2. Results

2.1. Full Polymeric Artificial Muscles

After electrogeneration, rinsing and drying the PPy films were peeled off from the supporting stainless steel electrode, cut in several strips, weighted, adhered to the tape (when required), and painted around with a narrow transversal paint strip close to the bilayer top: they are full polymeric devices not including any sputtered or deposited metallic film. The transversal paint strip tries to avoid the electrolyte contact, by capillarity, with the metal clamp: parallel electrolyte reactions at the metal clamp are avoided during current flow.[55,56] **Figure 1**(a) shows a schema of the studied bilayer muscles. Figure 1(b) shows a muscle in the cell and how the bending angle bellow the paint strip is determined.

2.2. Stationary Coulo-Voltammetric (*Q*/*E*) Responses

The PPy-ClO_4/PPy-DBS bilayer muscle was submitted to 40 consecutive voltammetric cycles between –0.8 and 0.5 V at

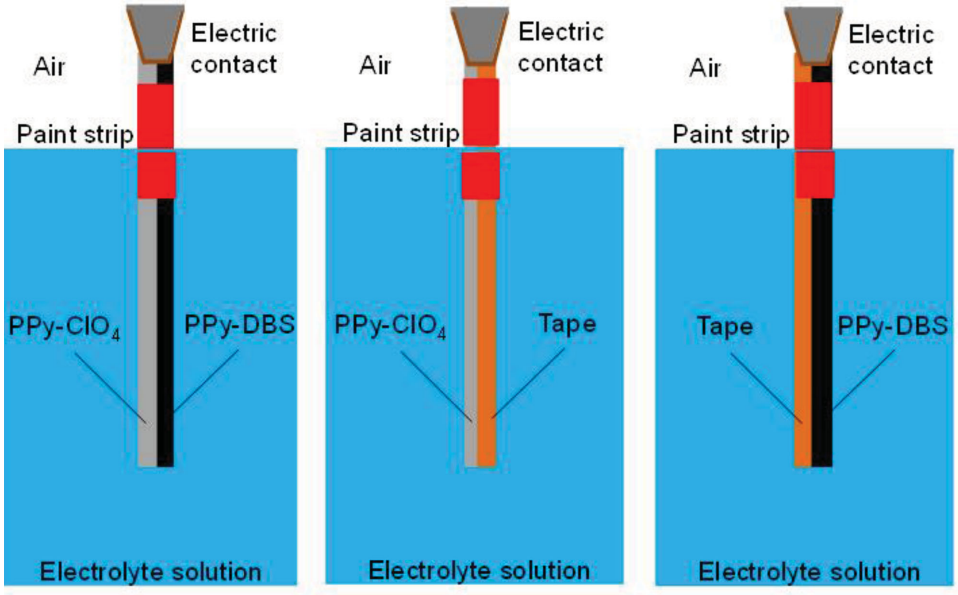

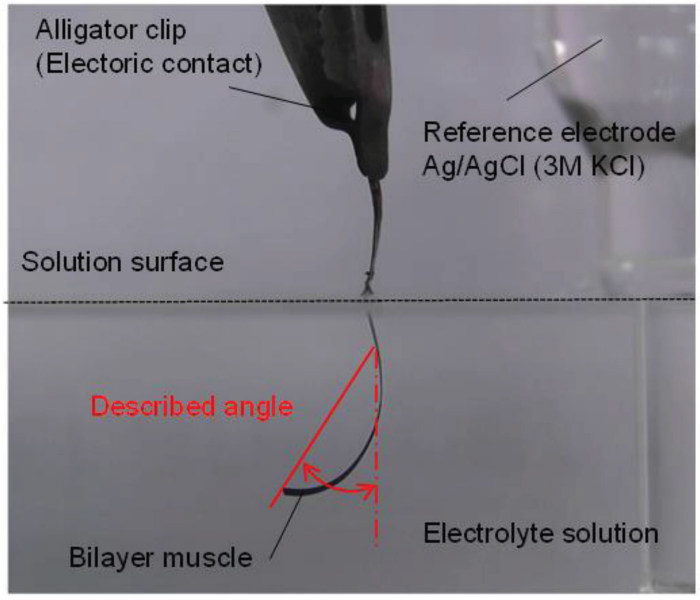

Figure 1. a) Scheme of the PPy-ClO_4/PPy-DBS, PPy-ClO_4/tape, and PPy-DBS/tape bilayer artificial muscles: layer's relative position, transversal paint strip, and electrical contact clamp metal alligator metal; b) Bilayer muscle in the cell and determination of the bending angle.

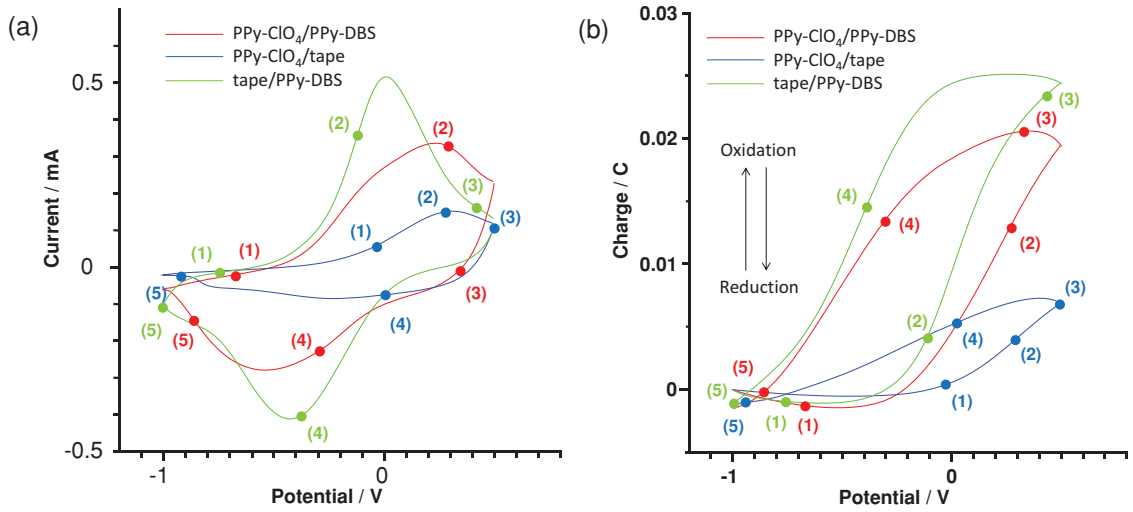

Figure 2. a) Stationary cyclic voltammetric (CV) responses between –1.0 V and 0.7 V at 10 mV s^{-1} in 0.5 M NaBr aqueous solution and at room temperature from the PPy-Br/PPy-DBS, PPy-Br/tape, and PPy-DBS/tape bilayer muscles; b) Coulo-voltammetric (Q/E) responses obtained by integration of the CV.

a scan rate of 10 mV s^{-1} in 0.5 M NaBr aqueous solution. The consecutive voltammograms present raising currents only getting stationary responses (consecutive voltammograms overlap) after 40 cycles. By cycling original ClO_4^- ions should be substituted in the film by the new anion present in the control electrolyte, Br^-, while the HDBS becomes NaDBS: the bilayer should become PPy-Br/PPy-DBS. On this way any previous structural memory[57–60] attained during the PPy electropolymerization processes was erased and the internal film structure (chains-ions-water) was readapted to the actual dynamic oxidation/reduction conditions. The working conditions (electrolyte concentration, temperature, initial and final potentials or potential sweep rate) can be changed then getting stationary voltammograms after only two consecutive cycles.

Figure 2(a) shows the stationary voltammetric responses from each of the three studied muscles: PPy-Br/PPy-DBS (red), PPy-Br/tape (Blue) and PPy-DBS/tape (green). The parallel bending movements were video recorded in order to get the angle described at every applied potential. By voltammetric integration the concomitant coulo-voltammetric (Q/E) responses, Figure 2(b), were attained showing practically closed Q/E loops: the oxidation charge equals the reduction charge indicating that the flowing charge is consumed by the reversible PPy oxidation/reduction reactions driven the muscle actuation.[55,61] Positive charge increments quantify PPy oxidation and negative increments, PPy reduction.

2.3. Artificial Muscles are Faradaic Motors

Figure 3 shows the concomitant evolutions of the bending angles, got from the video frames, as a function of the consumed electrical charge (α/Q plot) during the voltammetric sweep. **Figure 4** presents both, pictures taken from the recorded video frames and the parallel schemas indicating the described angle at each potential (points 1–5 were underlined).

The tape/PPy-Br (tape on the left side/PPy on the right side) bilayer muscle describes (Figure 4a) a clockwise angular movement during the full potential range of PPy oxidation (Figure 2b) indicating that the PPy film swells [53] by the oxidation driven entrance of anions (charge balance) and water (osmotic balance), corroborating the exchange of Br^- ions. Reduction charges (Figure 2b) give anticlockwise angular displacement (Figure 4a) corroborating that the PPy film shrinks by expulsion of Br^- and water. The voltammetric cycle drives a reversible angular movement of 30°. Coulo-dynamic (α/Q) results show (Figure 3a) that the described angle is close to a linear function of the oxidation and reduction consumed charges. Those results support the Faradaic origin of the muscle movement driven by the reaction:

$$\left[(Pol)^{m+}\left(A^-\right)_m(S)_o\right]_{gel} + n\left(A^-\right) + p(S) \underset{red}{\overset{ox}{\rightleftarrows}} \left[(Pol)^{(m+n)+}\left(A^-\right)_{m+n}(S)_{o+p}\right]_{gel} + n\left(e^-\right)_{metal} \quad (1)$$

being A^- the anions exchanged for charge balance, Br^- here; $(Pol)^{m+}$, the partially oxidized PPy film chains; S, the solvent molecules exchanged for osmotic balance; the sub-index gel indicates the nature of the film and ne^- represent the electrons exchanged for every chain oxidation/reduction. Volume variations required to lodge/expel n Br^- ions and p solvent molecules (and the concomitant described angles) are defined through the consumed charge, Q, by the number of exchanged monovalent Br^- ions ($n = Q/e^-$, being e^- the electron charge) and its ion's and water molecule's volume.[62]

During the device actuation the current flow promotes the PPy reaction, conformational movements of the chains (molecular motors[63] with generation/destruction of free volume required to exchange n Br^- ions and p water molecules. The consecutive events mimic, step by step, those taking place in natural muscles during actuation.[3,27,32,64]

The coulo-dynamic (α/Q) plot presents two hysteresis loops. The electrochemical reaction induces structural (relaxation, swelling, shrinking, closing, and conformational compaction)

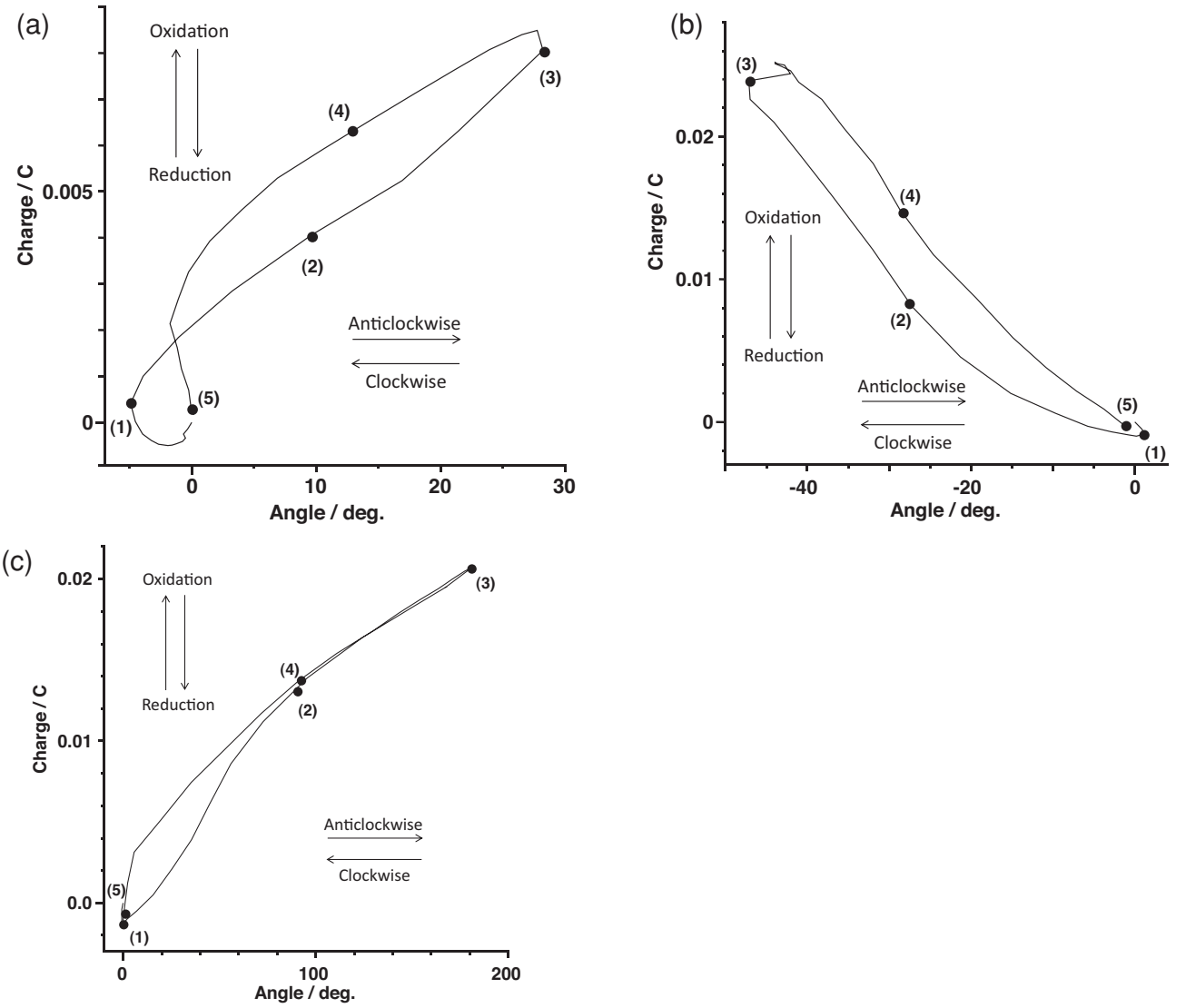

Figure 3. Angular displacement described by the three studied bilayer muscles as a function of the consumed charge during the voltammetric cycle a) PPy-Br/tape; b) PPy-DBS/tape, and c) PPy-Br/PPy-DBS.

changes in the film.[54,55,65] The reaction induced osmotic balance is a physical process: it follows or precedes the Faradaic exchange of Br^- ions adapting its rate to the reaction driven structural conditions. The hysteresis loops should indicate asymmetric (not parallel to anion) water entrance/exit adapted to the actual Br^- concentration in the film and to the reaction induced structural changes.[56,62,66–68] Thus, after oxidation completion the bending angle still increases (Figure 4a) when the PPy reduction starts: the PPy film osmotic swelling goes on by entrance of water driven by the high concentration of anions in the film while the anion's expulsion begins. The osmotic balance is delayed related to the Faradaic exchange of anions.

The film reduction drives consecutive film shrinking, closing its structure (when the average distance between chains fits the diameter of the anion unit) trapping over 30% of the counterions (Br^-), and conformational compacting.[52] Figure 3 points to a faster electro-osmotic expulsion of water around the closing potential: when the average "pore" diameter fits the ion diameter the moving Br^- ions drag the solvent in front of it, as ions do during paint electrodepositions.[69] Under steady state conditions (balanced charge and osmotic pressure) the angular displacement of a muscle in different electrolytes allows the quantification of the number of water molecules exchanged per reaction unit.[62,70,71] In biochemical processes this a key number determining health or diseases that still cannot be determined.

The tape/PPy-DBS bilayer muscle describes (Figure 3b) anticlockwise angular displacement during oxidation (Figure 2b) corroborating that the PPy-DBS film shrinks by oxidation with expulsion of Na^+ and water.[72] Reduction charges (Figure 2b) give clockwise angular displacements indicating the PPy swelling by reduction with entrance of cations and water. A reversible bending movement of 50 degrees is described during the oxidation/reduction cycle (Figure 3b) being the described angle a linear function of the consumed charge: this is a Faradaic muscle driven by the reaction:

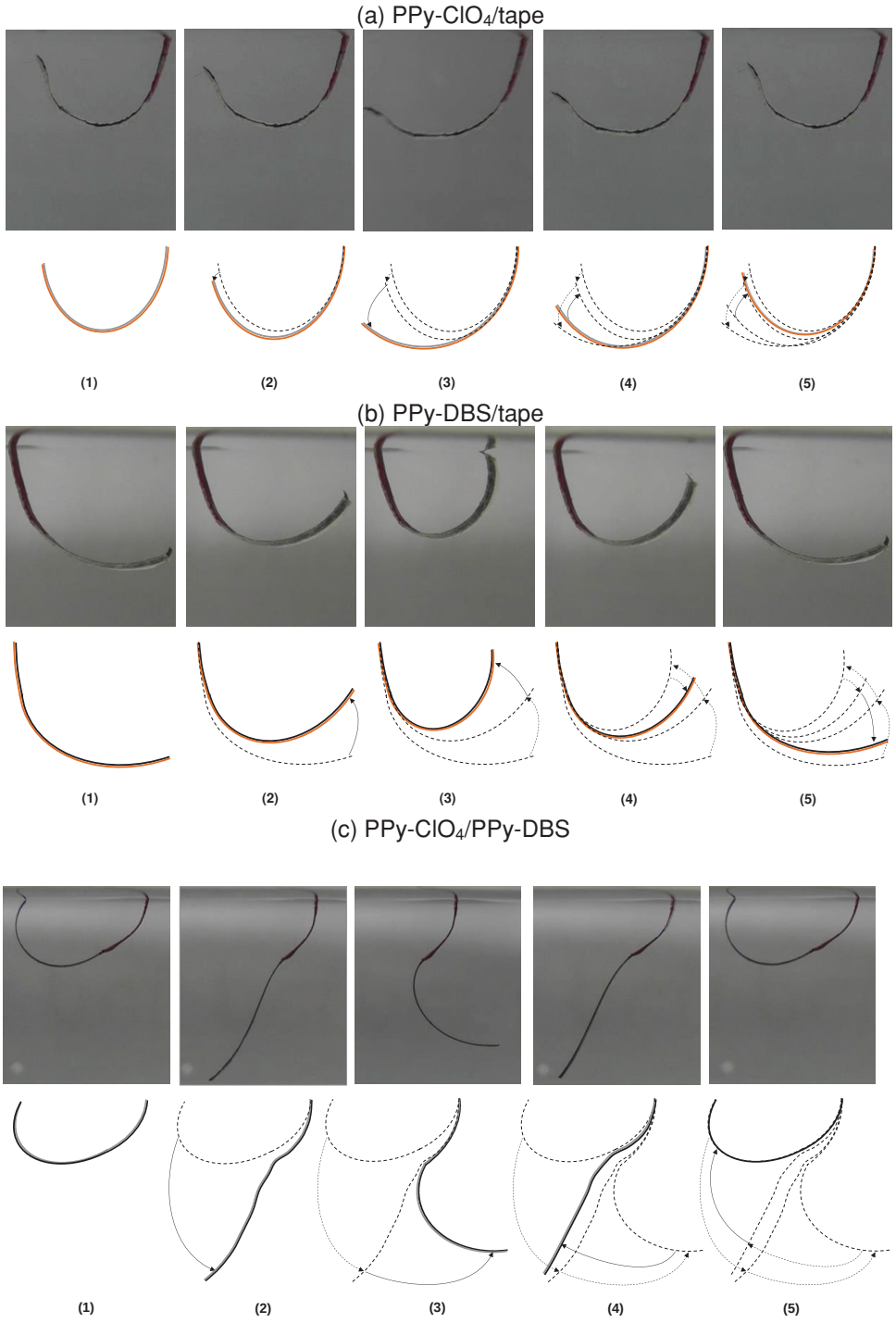

Figure 4. Pictures and schemes of the angular displacements described by the different bilayers artificial muscles: a) PPy-Br/tape, b) PPy-DBS/tape, and c) PPy-Br/PPy-DBS at the potentials corresponding to points (1), (2), (3), (4), and (5) on the voltammetric and coulo-voltammetric responses from figure 2.

$$\left[(Pol)^{(m-n)+}\left(MA^{-}\right)_{m-n}\left(C^{+}\right)_{n}(S)_{o+p}\right]_{\text{gel}} \underset{\text{red}}{\overset{\text{ox}}{\rightleftarrows}} \left[(Pol)^{m+}\left(MA^{-}\right)_{m}(S)_{o}\right]_{\text{gel}} + n\left(C^{+}\right) + p(S) + n\left(e^{-}\right)_{\text{metal}} \quad (2)$$

where MA^{-} is the macro-anion (DBS^{-} here) trapped inside the PPy film during electrogeneration of PPy^{n+} (oxidized chains) and C^{+} represents the exchanged cation, Na^{+} here.

The small hysteresis loop seems related to the asymmetric water entrance/exit following reaction induced structural changes and Na^+ exchanges.

As expected from the driving reactions 1 and 2 the PPy-Br/PPy-DBS bilayer muscle describes a clockwise bending movement during oxidation (Figure 3c): the PPy-Br film swells by entrance of anions and water (reaction 1, forwards) and the PPy-DBS film shrinks by expulsion of cations and water (reaction 2, forwards). During the bilayer reduction the muscle describes anticlockwise bending movement driven by the opposed layer reactions and ionic movements. The described reversible angle during the potential cycle is (Figure 3c) 200 degrees. The bilayer is a Faradaic muscle: the described angle is a linear function of the consumed charge[43] through reactions 1 and 2. The amplitude of the described movement is now over 6 times the amplitude described by the PPy-Br/tape bilayer and over 4 times that of the PPy-DBS/tape bilayer in the same electrolyte for the same potential sweep range.

The bilayer muscle oxidation drives a simultaneous and asymmetric shrinking/swelling: the PPy-Br layer swells (reaction 1, forwards) and pushes the bilayer and the PPy-DBS layer shrinks (reaction 2, forwards) and pulls the bilayer. Its reduction drives the simultaneous asymmetric swelling/shrinking. Reaction driven structural asymmetries originates a cooperative (synergic) electro-chemo-mechanical actuation (bending).

At the PPy-Br/tape and tape/PPy-DBS bilayer muscles the PPy film is the only reactive (reaction driven swelling/shrinking) layer during actuation: the only one pushing or pulling the device. The tape acts as a passive film (necessary for the generation of the transversal stress actuation) but consuming energy to be bended (bending energy) and trailed (gravimetric energy). The asymmetric and cooperative reactivity in the PPy-Br/PPy-DBS bilayer promotes a cooperative asymmetric pushing/pulling mechanical effect. The result is a magnification of the angular displacement related to that of each PPy/tape bilayer muscles. The cooperative dynamic effect can be quantified by the angle (degrees) described per unit of consumed charge (mC): 2,35; 0.34, and 0.52 (° mC^{-1}) for the PPy-Br/PPy-DBS, PPy-Br/tape and tape/PPy-DBS bilayers, respectively.

3. Conclusion

As conclusion, full conducting polymer asymmetric bilayer muscles produce cooperative and synergic electro-chemo-mechanical actuation. The optimum asymmetric cooperation is attained when one of the films exchanges anions swelling/shrinking during its respective oxidation/reduction reactions and the second film exchanges cations inducing shrinking/swelling during oxidation/reduction, respectively. The cooperative effect is due to the asymmetric simultaneous swelling/shrinking processes driven by the simultaneous oxidation of the two films and the concomitant reverse asymmetric shrinking/swelling driven by the two film's reduction: one of the layers pushes the device and the second layer pulls it. The asymmetric bilayer is a Faradaic motor (driven by electrochemical reactions): the bending angle is a linear function of the consumed charge. The amplitude of the movement (described angle for bending muscles) per unit of consumed charge quantifies the cooperative mechanical actuation. The asymmetric PPy-Br/PPy-DBS bilayer muscle is 7 or 4 times most efficient than the PPy-Br/tape and tape/PPy-DBS bilayer muscles, respectively. Small coulo-dynamic loops were related to asymmetric osmotic and electro-osmotic processes under reaction structural control.

4. Experimental Section

Pyrrole (Fluka) was purified by distillation under vacuum using a diaphragm vacuum pump (MZ 2C, SCHOTT) and stored in cold at –15 °C. Sodium bromide (NaBr, Sigma–Aldrich), Lithium perchlorate ($LiClO_4$, Fluka), and Dodecylbenzenesulfonic acid solution 70 wt% in isopropanol (DBSA, Aldrich) were used as received. Ultrapure water from Millipore Milli-Q equipment was used.

All the electrochemical experiments were performed in a three electrodes electrochemical cell using a potentiostat-galvanostat Autolab PGSTAT100, controlled with a personal computer through GPES electrochemical software. As reference electrode for every experiment a Metrohm Ag/AgCl (3M KCl) was used. Every potential in this work is referred to this electrode. The polymeric films mass and thickness were obtained by using a Sartorious SC2 balance ($\pm 10^{-7}$ g) and an electronic micrometer (±1 μm) from COMECTA, respectively. Movement of the bilayer was recorded using a digital video camera DMC-FX77, Panasonic.

The electrogeneration of PPy-ClO_4 and PPy-DBS films was described in previous works.[7,34]

A stainless steel working electrode was first coated with a polypyrrole-dodecylbenzenesulfonic acid (PPy-DBS) film following the procedure described in reference.[7] The coated electrode was then rinsed with pure water and was dried in a glass box containing silica gel (Panreac) for 3 days. After that, the dry PPy-DBS coated steel electrode was immersed in 50 mL of a 0.10 M $LiClO_4$ and 0.20 M pyrrole aqueous solution and a PPy-ClO_4 film was electrogenerated following the procedure described in reference.[34] Once generated the PPy-ClO_4/PPy-DBS bilayer was rinsed with water and dried in air at room temperature during 1 day. Once dried, the borders of the working electrode were scrapped and the two PPy-ClO_4/PPy-DBS bilayer films (one by side) were peeled off from the steel electrode. Those films were cut into smaller strips each 20 × 1 mm, and 50 μm thick, weighing 0.78 ± 0.01 mg. A transversal paint strip, from 5.0 mm to 12.0 mm of the top, will avoid electrolyte capillarity to the metal contact. Each of the bilayer actuators was characterized in 0.5 M NaBr aqueous solutions by cyclic voltammetry.

Acknowledgements

The authors acknowledge the financial support from the Kyushu Institute of Technology and the Spanish Government (MCINN) Projects MAT2011–24973. J.G.M. acknowledges Spanish Education Ministry for a FPU grant (AP2010–3460).

Received: November 17, 2014
Revised: January 9, 2015
Published online: January 29, 2015

[1] C. Jo, D. Pugal, I.-K. Oh, K. J. Kim, K. Asaka, *Prog. Polym. Sci.* **2013**, *38*, 1037.
[2] I. J. Busch-Vishniac, *Electromech. Sens. Actuators* Springer-Verlag, Berlin, **1999**.
[3] T. F. Otero, J. G. Martinez, J. Arias-Pardilla, *Electrochim. Acta* **2012**, *84*, 112.
[4] T. F. Otero, in *Mod. Asp. Electrochem.* (Eds: R. E. White, J. O. Bockris, B. E. Conway), Springer US, New York **1999**, pp 307–434.

[5] T. F. Otero, M. T. Cortes, *Chem. Commun.* **2004**, 284.
[6] T. F. Otero, J. M. Sansiñena, *Bioelectrochem. Bioenerg.* **1997**, *42*, 117.
[7] L. V. Conzuelo, J. Arias-Pardilla, J. V. Cauich-Rodríguez, M. A. Smit, T. F. Otero, *Sensors* **2010**, *10*, 2638.
[8] Q. Pei, O. Inganas, *J. Phys. Chem.* **1992**, *96*, 10507.
[9] Q. Pei, O. Inganas, *J. Phys. Chem.* **1993**, *97*, 6034.
[10] Q. Pei, O. Inganas, *Solid State Ion.* **1993**, *60*, 161.
[11] M. Christophersen, B. Shapiro, E. Smela, *Sens. Actuators B Chem.* **2006**, *115*, 596.
[12] G. Alici, B. Mui, C. Cook, *Sens. Actuators A Phys.* **2006**, *126*, 396.
[13] G. Alici, N. N. Huynh, *Sens. Actuators A Phys.* **2006**, *132*, 616.
[14] G. Alici, G. Spinks, N. N. Huynh, L. Sarmadi, R. Minato, *Bioinspir. Biomim.* **2007**, *2*, S18.
[15] P. Du, X. Lin, X. Zhang, *Sens. Actuators A Phys.* **2010**, *163*, 240.
[16] G. Alici, P. Metz, G. M. Spinks, *Smart Mater. Struct.* **2006**, *15*, 243.
[17] P. Metz, G. Alici, G. M. SpinkS, *Sens. Actuators A Phys.* **2006**, *130*, 1.
[18] B. Shapiro, E. Smela, *J. Intell. Mater. Syst. Struct.* **2007**, *18*, 181.
[19] G. Paasch, *Electrochem. Commun.* **2000**, *2*, 371.
[20] W. Albery, A. Mount, *J. Chem. Soc. Faraday Trans.* **1993**, *89*, 327.
[21] J. Bisquert, G. G. Belmonte, F. F. Santiago, N. S. Ferriols, M. Yamashita, E. C. Pereira, *Electrochem. Commun.* **2000**, *2*, 601.
[22] X. M. Ren, P. G. Pickup, *J. Electroanal. Chem.* **1997**, *420*, 251.
[23] Y. Fang, X. Tan, Y. Shen, N. Xi, G. Alici, *Mater. Sci. Eng. C-Biomim. Supramol. Syst.* **2008**, *28*, 421.
[24] T. Shoa, J. D. W. Madden, N. R. Munce, V. Yang, *Polym. Int.* **2010**, *59*, 343.
[25] G. Alici, *Sens. Actuators B Chem.* **2009**, *141*, 284.
[26] R. Verdu, R. Berenguer, J. Morales, G. Vazquez, T. F. Otero, L. Weruaga, in *2005 Int. Conf. Image Process. ICIP Vols 1–5*IEEE, New York, **2005**, pp 3705–3708.
[27] T. F. Otero, J. G. Martinez, *Prog. Polym. Sci.* **2014**, DOI:0.1016/j.progpolymsci.2014.09.002.
[28] T. Otero, M. Cortes, *Adv. Mater.* **2003**, *15*, 279.
[29] T. F. Otero, M. T. Cortes, *Sens. Actuators B Chem.* **2003**, *96*, 152.
[30] J. A. Ashton-Miller, E. M. Wojtys, L. J. Huston, D. Fry-Welch, *Knee Surg. Sports Traumatol. Arthrosc.* **2001**, *9*, 128.
[31] J. R. Lackner, P. DiZio, in *Annu. Rev. Psychol.* Annual Reviews, Palo Alto **2005**, pp 115–147.
[32] T. F. Otero, J. J. Sanchez, J. G. Martinez, *J. Phys. Chem. B* **2012**, *116*, 5279.
[33] J. G. Martinez, T. F. Otero, *J. Phys. Chem. B* **2012**, *116*, 9223.
[34] T. F. Otero, E. Angulo, J. Rodríguez, C. Santamaría, *J. Electroanal. Chem.* **1992**, *341*, 369.
[35] Q. Pei, O. Inganas, *Adv. Mater.* **1992**, *4*, 277.
[36] E. Smela, O. Inganas, Q. Pei, I. Lundstrom, *Adv. Mater.* **1993**, *5*, 630.
[37] E. W. H. Jager, E. Smela, O. Inganas, *Science* **2000**, *290*, 1540.
[38] E. W. H. Jager, O. Inganas, I. Lundstrom, *Science* **2000**, *288*, 2335.
[39] S. J. Higgins, K. V. Lovell, R. M. G. Rajapakse, N. M. Walsby, *J. Mater. Chem.* **2003**, *13*, 2485.
[40] N. Festin, C. Plesse, P. Pirim, C. Chevrot, F. Vidal, *Sens. Actuators B Chem.* **2014**, *193*, 82.
[41] F. Vidal, J. F. Popp, C. Plesse, C. Chevrot, D. Teyssie, *J. Appl. Polym. Sci.* **2003**, *90*, 3569.
[42] M. Fuchiwaki, K. Tanaka, K. Kaneto, *Sens. Actuators Phys.* **2009**, *150*, 272.
[43] M. Fuchiwaki, T. F. Otero, *J. Mater. Chem. B* **2014**, *2*, 1954.
[44] T. Okamoto, K. Tada, M. Onoda, *Jpn. J. Appl. Phys. Part 1-Regul. Pap. Short Notes Rev. Pap.* **2000**, *39*, 2854.
[45] M. Onoda, T. Okamoto, K. Tada, H. Nakayama, *Jpn. J. Appl. Phys. Part 2 Lett.* **1999**, *38*, L1070.
[46] M. Onoda, K. Tada, *Ieice Trans. Electron.* **2004**, *E87C*128.
[47] M. Onoda, K. Tada, H. Nakayama, *Synth. Met.* **1999**, *102*, 1321.
[48] S. Shakuda, S. Morita, T. Kawai, K. Yoshino, *Jpn. J. Appl. Phys. Part 1 Regul. Pap. Short Notes Rev. Pap.* **1993**, *32*, 5143.
[49] W. Takashima, S. S. Pandey, K. Kaneto, *Synth. Met.* **2003**, *135*, 61.
[50] W. Takashima, S. S. Pandey, K. Kaneto, *Sens. Actuators B Chem.* **2003**, *89*, 48.
[51] T. F. Otero, *Polym. Rev.* **2013**, *53*, 311.
[52] T. F. Otero, J. G. Martinez, *Adv. Funct. Mater.* **2014**, *24*, 1259.
[53] T. F. Otero, J. G. Martinez, *Sens. Actuators B Chem.* **2014**, *199*, 27.
[54] T. F. Otero, J. G. Martinez, M. Fuchiwaki, L. Valero, *Adv. Funct. Mater.* **2014**, *24*, 1265.
[55] T. F. Otero, M. Alfaro, V. Martinez, M. A. Perez, J. G. Martinez, *Adv. Funct. Mater.* **2013**, *23*, 3929.
[56] J. G. Martinez, T. F. Otero, E. W. H. Jager, *Langmuir* **2014**, *30*, 3894.
[57] B. Villeret, M. Nechtschein, *Phys. Rev. Lett.* **1989**, *63*, 1285.
[58] T. Sendai, H. Suematsu, K. Kaneto, *Jpn. J. Appl. Phys.* **2009**, *48*, 051506.
[59] M. A. Vorotyntsev, M. Skompska, E. Pousson, J. Goux, C. Moise, *J. Electroanal. Chem.* **2003**, *552*, 307.
[60] J. Heinze, A. Rasche, *J. Solid State Electrochem.* **2006**, *10*, 148.
[61] H. Grande, T. F. Otero, *J. Phys. Chem. B* **1998**, *102*, 7535.
[62] T. F. Otero, J. G. Martinez, *Chem. Mater.* **2012**, *24*, 4093.
[63] T. F. Otero, H. Grande, J. Rodriguez, *J. Phys. Org. Chem.* **1996**, *9*, 381.
[64] T. F. Otero, J. G. Martinez, *J. Mater. Chem. B* **2013**, *1*, 26.
[65] T. Otero, H. Grande, J. Rodriguez, *J. Electroanal. Chem.* **1995**, *394*, 211.
[66] C. Jo, H. E. Naguib, R. H. Kwon, *Smart Mater. Struct.* **2011**, *20*, 045006.
[67] M. J. M. Jafeen, M. A. Careem, S. Skaarup, *Ionics* **2010**, *16*, 1.
[68] K. P. Vidanapathirana, M. A. Careem, S. Skaarup, K. West, *Solid State Ion.* **2002**, *154*, 331.
[69] W. Machu, *Handbook of Electropainting Technology* Electrochemical Publications Limited, Glasgow **1978**.
[70] T. F. Otero, J. G. Martínez, B. Zaifoglu, *Smart Mater. Struct.* **2013**, *22*, 104019.
[71] L. Valero, T. F. Otero, J. G. Martínez, *ChemPhysChem* **2014**, *15*, 293.
[72] L. Valero, J. Arias-Pardilla, J. Cauich-Rodríguez, M. A. Smit, T. F. Otero, *Electrochim. Acta* **2011**, *56*, 3721.